

# **A Refined Conceptual Model for Subsidence at Wairakei, New Zealand**

**Fabian Sepulveda<sup>1</sup>, Chris J. Bromley<sup>2</sup>, Fabian Hanik<sup>1</sup>,  
Paul F. Bixley<sup>1</sup>, Abdul Nishar<sup>1</sup>, Warren Mannington<sup>1</sup>**

<sup>1</sup>Contact Energy Ltd, Taupo, New Zealand

<sup>2</sup>GNS Science, Wairakei, Taupo, New Zealand

## **Keywords**

*Wairakei, subsidence, benchmark level history, swelling clay, sigmoidal curve fitting, pressure trends, compressible layer*

## **ABSTRACT**

Production of geothermal fluid started at Wairakei in the 1950's with subsidence being one surface effect observed as a result of production. Large-scale reinjection was implemented in the late 1990's. Thanks to an extensive levelling benchmark network, it has been possible to thoroughly monitor benchmark level history at Wairakei throughout its operating history (period 1952-2017). At the center of the area of high subsidence (referred to as Wairakei Bowl), surface level has dropped in excess of 15 m. Previous studies attributed subsidence to compaction of shallow, clay-rich sediments capping the geothermal system (Allis, 2000), and showed that within the area of subsidence, some benchmark level history can be approximated by a sigmoidal curve (Bromley, 2006). In this study, level history until 2017 is studied for selected benchmarks of the Wairakei Bowl using multiple sigmoidal curve fitting with input parameters calibrated against field pressure history and thickness and depth of the compacting layer(s). The latter are re-interpreted using vertical shifts in well casing coupling depths and swelling clay anomalies. It is shown that benchmarks show a general reduction in subsidence rate with time as dictated by sigmoidal trends, with second-order variations in subsidence rate controlled by pressure trends in the reservoir.

## **1. Introduction**

### ***1.1 Field operating history***

A detailed account of pre-2009 production history of Wairakei can be found in Bixley et al. (2009). In this section, production history until 2016 is briefly described. All geographic areas and power stations mentioned in this section (Te Mihi, EBF, WBF, Poihipi, Otupu and Karapiti) are shown in Figure 1. The Wairakei geothermal field has been in commercial operation since

1958, which is the longest operating history of a liquid-dominated field worldwide. Fluid extraction started in the EBF and moved progressively west through WBF to Te Mihi. The Poihipi Power Station (55 MWe installed capacity; commissioned in 1995) utilized initially dry-steam wells from the Poihipi production area. In 1998, large-scale reinjection of separated brine started at Wairakei in the Otupu area. In 2012, following changes to the Te Mihi steamfield, the Poihipi Power Station was able to operate with a mixed steam input from both Poihipi and Te Mihi wells. This change resulted in an increased fluid take from the Te Mihi reservoir. Commissioning of Te Mihi Power Station (166 MWe installed capacity) in 2014 led to a further increase in mass take from Te Mihi. The additional reinjection capacity required as a result of increased Te Mihi fluid take (period 2012-2014) was sourced from new Otupu wells and commissioning of the Karapiti reinjection area in 2011. Presently, Wairakei is the largest operating geothermal field in New Zealand, with a current installed capacity in excess of 370 MWe (Figure 1).

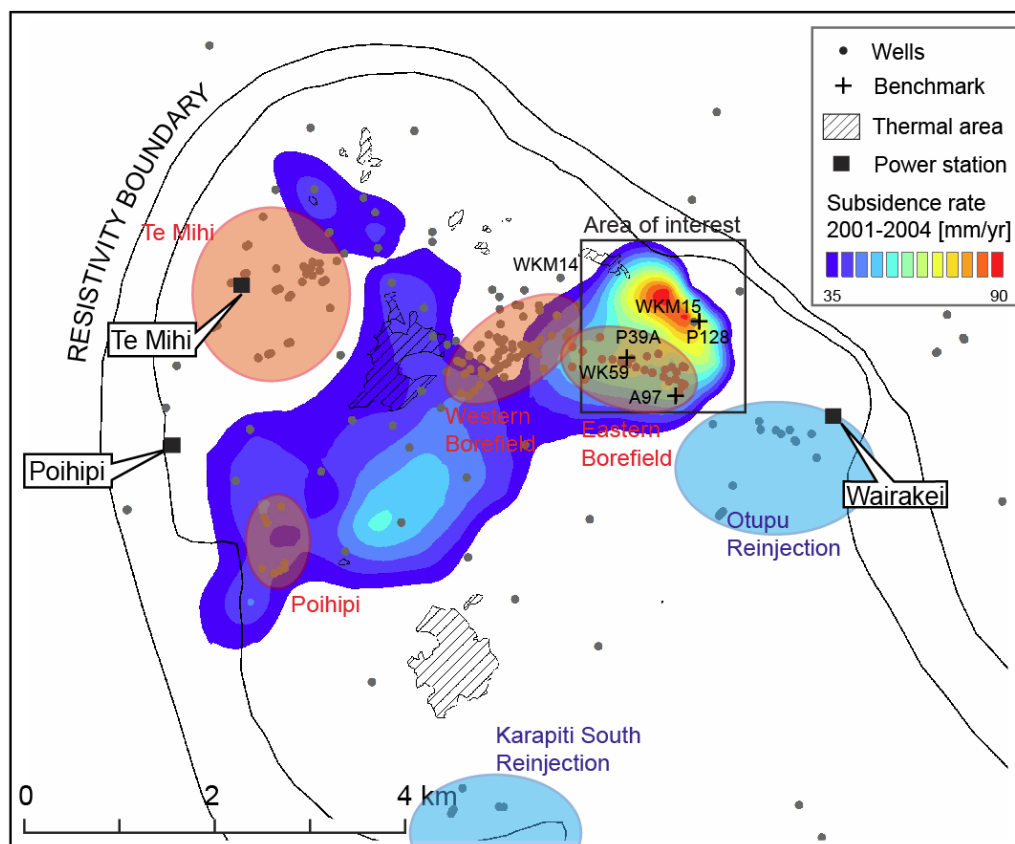


**Figure 1:** Map showing Wairakei geothermal field, areas of subsidence and selected benchmarks and wells discussed in this study. Production areas shown by red circles. EBF = Eastern Borefield; WBF = Western Borefield. Thermal area within area of interest to the northwest of Wairakei Bowl corresponds to extinct area of boiling chloride-spring discharge.

## 1.2 Subsidence at Wairakei

Among early surface effects of production were pressure drawdown (Bixley *et al.*, 2009), extinction of chloride boiling springs (White and Hunt, 2005) and development of subsidence in the Wairakei area (Allis, 2000; Allis and Zhan, 2000; Allis *et al.*, 2009; Bromley, 2006; Bromley

et al., 2010, 2013, 2015). Figure 1 provides a snapshot of subsidence rates for the period 2001-2004 highlighting areas of relatively high subsidence. At the center of high subsidence areas, cumulative subsidence of up to 15 m has been measured (e.g. benchmark P128 at Wairakei). The main area of high subsidence at Wairakei, referred to as “Wairakei Bowl”, falls within the “area of interest” in Figure 1.

The geology of the Wairakei-Tauhara geothermal field is described in detail by Rosenberg et al. (2009) and Bignall et al. (2010). Shallow (<400 mGL; “meters below ground level”) geological formations relevant to the understanding of subsidence include, from top to bottom: Superficial deposits (collectively including Alluvium, Taupo Ignimbrite and Oruanui Formation); Huka Falls Formation (HFF; including Upper HFF, Mid HFF, and Lower HFF), and Upper Waiora Formation (Upper WF). Upper and Lower HFF units are mostly composed of fine-grained lacustrine sediments which act as a relatively impermeable cap for the deep geothermal system (Rosenberg et al., 2009). Upper and Lower HFF units, collectively referred to as “clay cap”, are separated by a relatively permeable volcanic breccia (Mid HFF). The following geo-hydrological units are identified for this study: Groundwater aquifers (above HFF), mid-HFF aquifer (this may include 2-phase and liquid aquifers), and Lower HFF-Upper WF aquifers (this may include 2-phase and liquid aquifers).

Among the main hypotheses explaining subsidence at Wairakei are those by Allis (2000) and Bromley (2006) including:

1. Presence of relatively compressible “geothermal clays” or “geothermally-modified mudstones” within Upper HFF and Lower HFF units;
2. Pressure drawdown in the WF liquid reservoir diffusing slowly upwards through the clay cap.

Bromley (2006) also showed that long-term benchmark level history, such as that of benchmark P128 located near the center of the Wairakei bowl; Figure 1), could be reasonably matched by a sigmoidal curve (also referred to as Boltzmann function) of the form:

$$S(t) = s'(t) \left( 1 - \frac{1}{1 + e^{\frac{t-T_0}{T_1}}} \right) \quad (1)$$

where:

$$s'(t) = s_{\max} \frac{(t - T_{\text{start}})}{(T_{\text{end}} - T_{\text{start}})} \quad (2)$$

where  $t$  is time in years,  $S(t)$  is cumulative subsidence in meters at time  $t$ , and  $s'(t)$  is a linear function (for  $T_{\text{start}} < t < T_{\text{end}}$ ) of subsidence, where  $T_{\text{start}}$  and  $T_{\text{end}}$  are the approximate start and end time of the period of deep reservoir pressure decline. The second term in brackets in equation (1) is a diffusive exponential term that delays and broadens the subsidence response, with the degree of spreading dictated by a diffusion time constant  $T_1$ , where  $T_0$  is the middle time ( $h(t) = \frac{1}{2} h_{\max}$ ; ignoring linear term). It can be shown that the exponential term alone in equation (1) is symmetric with respect to  $T_0$  (pivot point). The combination of a linear and exponential term

matches the common observation of level history where the tail end is broader than the roll off at the start (e.g. Figure2; Bromley, 2010).

In this paper, we review benchmark level history for the period 1952-2017 for selected benchmarks of the Wairakei Bowl, characterise changes in subsidence rate against various sigmoidal curve fitting models, and refine conceptual models of subsidence in the light of available reservoir information and field pressure history.

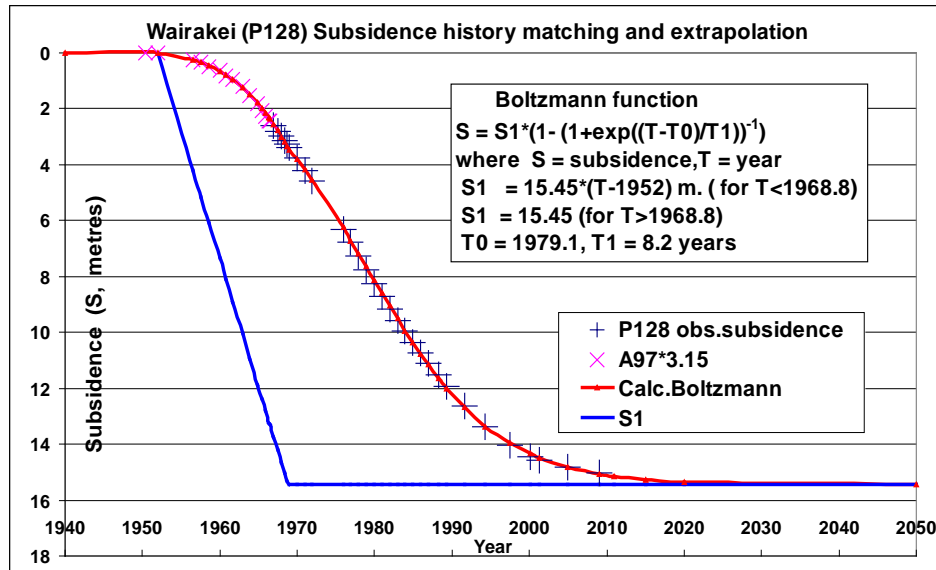


**Figure 2: Wairakei measured subsidence at P128, back-calculated prior to 1966 using A97 data. Total subsidence (m) extrapolated from 2004 to 2050 by fitting sigmoidal (Boltzmann) function (from Bromley et al., 2010).**

## 2. Data and methods

### 2.1 Well information

#### 2.1.1 Reservoir pressures

The deep liquid reservoir underwent a pressure drawdown of up to 25 bar as a result of fluid extraction as measured in Waiora Formation (Figure 3; Bixley, 2009). This pressure drawdown created a two-phase zone through boiling at the top of Waiora Formation. Pressure drawdown propagated into shallow formations as demonstrated by groundwater level drops of tens of meters (e.g. Bromley et al., 2009) and decline in steam pressures of mid HFF (Bixley et al., 2009; Figure 3).

As a result of Otupu reinjection (1998), pressure recovery of up to 4 bars was observed in the Waiora Formation liquid reservoir (Bixley et al., 2009; Figure 3). During the post-1998 WF pressure recovery event, shallower reservoir pressures (i.e. Upper WF and Mid HFF) may have had a minor recovery as well although a conclusive assessment is not possible due to lack of

mid-HFF pressure data (Figure 3). As of 2012, following increased Te Mihi fluid extraction, WF liquid pressures saw a new increase in the rate of pressure decline (Figure 3).

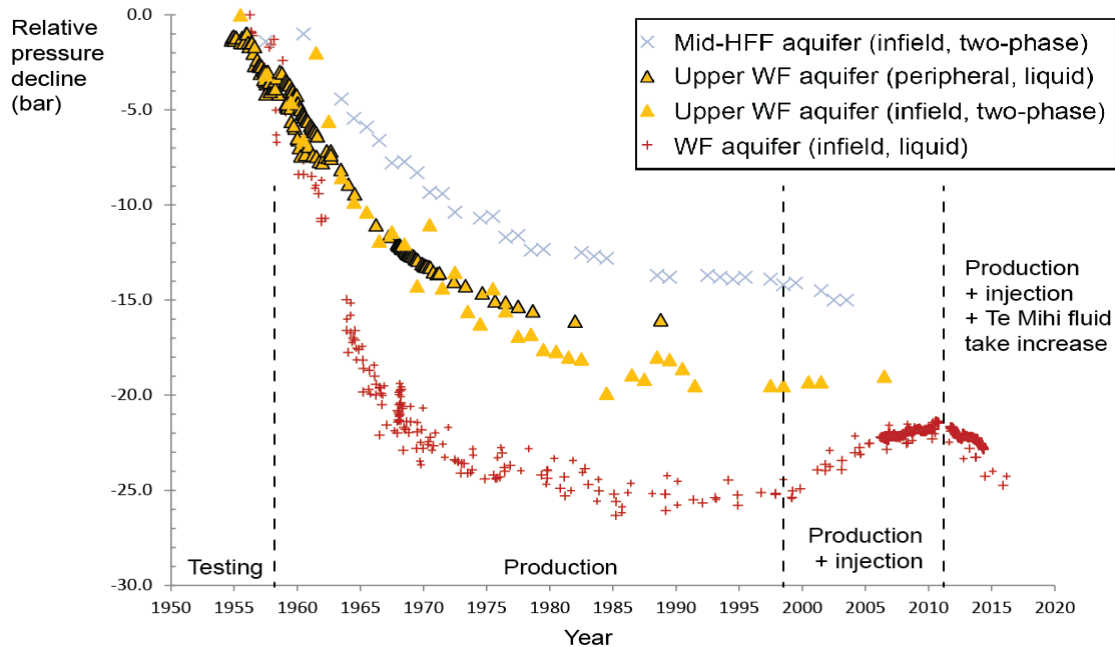


**Figure 3: Relative pressure change for mid HFF, Upper WF and WF wells over the period 1955-2017. Depth interval of aquifers shown in Figure 5.**

### 2.1.2 WK059 casing tallies

Well integrity assessments are undertaken on a routine basis at Wairakei to support decisions relating to well maintenance and abandonment. One of the risk factors to well casing integrity is cumulative subsidence. Allis *et al.* (2009) plotted casing deformation depths for selected Wairakei wells within areas of high subsidence and showed a peak of casing deformation depths within HFF. The likelihood of casing deformation may increase in the presence of corrosive fluids and/or weak casing cement bond strength. For the general case, however, casing deformation can be ascribed to compaction-induced stress where deformation depths represent a discrete point within the compacting layer. In this paper, a case study (well WK059) is presented where casing coupling shifts can be used in combination with swelling clay anomalies (further described in Section 2.1.3 below) to constrain the thickness of the compacting layer.

WK059 was drilled as a production well in 1958, decommissioned in 2014 and abandoned in 2017, following High-Temperature-Casing-Corrosion (HTCC) and camera inspections that identified casing obstructions at 188 and 162 m depth, respectively. Casing tallies compiled as part of the HTCC log were compared against original casing tallies. This comparison revealed a shift in casing coupling depths starting at approximately 100 mGL and reaching a cumulative shift of approximately 2 m at 171 m (Figure 4). Although HTCC casing coupling depths are not available past the deepest casing obstruction (188 m), it is possible to constrain the top depth of compacting layer (~100 m), which is in close coincidence with the top of the swelling clay layer as mapped in WKM15 (Figure 5; See Section 2.1.3 for details). It is anticipated that the coupling

shift curve would level off near the bottom of the compacting layer (Figure 4), which can be estimated from ground subsidence for the period 1958 (drill date) and 2014 (HTCC log date) measured at neighboring benchmark P39A (see section 2.2 for further details).

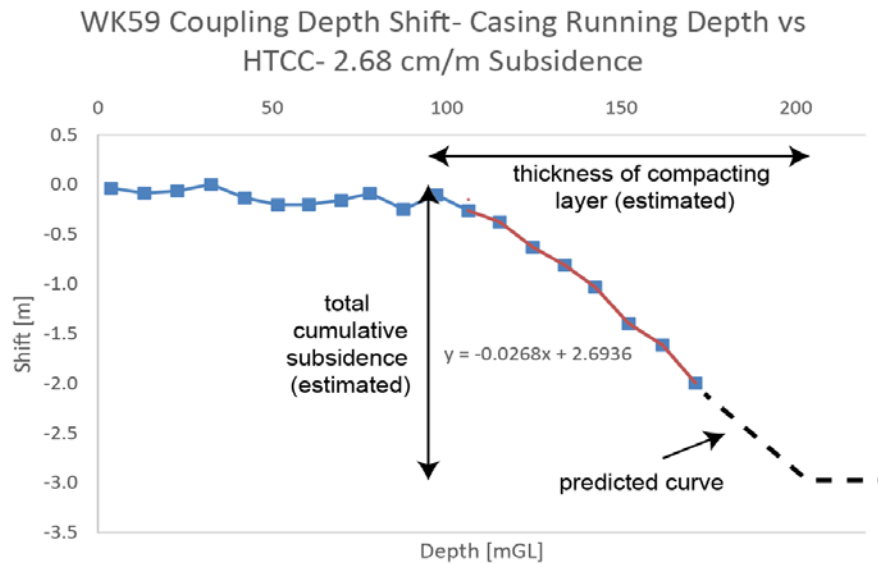


**Figure 4: WK059 Coupling Depth Shift- Casing Running Depth vs HTCC. A subsidence of- 2.68 cm/m is estimated from approximately 100 m to 171 m depth. mGL = meters below ground level.**

### 2.1.3 Well geology and alteration

Figure 5 presents a series of geological logs approximately arranged West (Left) to East (Right) near the main Wairakei subsidence areas, to illustrate the vertical and lateral extent of HFF. The various hydrological units referred to in Figure 3 are highlighted.

Swelling clays (including montmorillonite, smectite, and illite-smectite; e.g. Gunderson et al., 2000), as the name suggests, are prone to volume change due to their ability to incorporate or expel water into/out of their mineral structure, in response to pressure changes (e.g. Taylor and Smith, 1986; Villar and Smit, 2004). Other interesting properties of swelling clays include electrical conductivity and temperature dependence (e.g. Gunderson et al., 2000). At Wairakei, a close correlation was noted between swelling clay and the 100°-220°C isotherm range (Sepulveda et al., 2012). Lateral and vertical variations in swelling clay distribution and intensity at Wairakei are evident from Figure 5. During 2009, wells WKM14 (edge of subsidence area) and WKM15 (near center of the 15m subsidence anomaly area; Figure 1) were drilled as part of subsidence investigations (e.g. Bromley et al., 2010; Brockbank et al., 2011). Two high-swelling clay layers were measured in WKM15 at the depths of Upper HFF and Lower HFF-WF interface, respectively, with the greatest swelling clay concentrations in the Upper HFF layer. One main high-swelling clay layer was detected in WKM14 at the depth of Oruanui Formation-Upper HFF (Bromley et al., 2010; Sepulveda et al., 2012; Figure 5). Compressibility tests performed on core samples from WKM15 identified anomalously compressible material in Upper HFF and Upper WF (Bromley et al., 2010). The presence of high contents of swelling clays that are highly compressible suggested to Bromley et al. (2010) that intense hydrothermal

alteration of Upper HFF and Upper WF played a role in the localization of the Wairakei subsidence anomalies. Also, as documented in Sepulveda *et al.* (2012) and Correa *et al.* (2013), Otupu reinjection area (Figure 1) is characterized by comparatively weaker and deeper swelling clay anomalies (e.g. well WK317; Figure 5). Cumulative subsidence of the Otupu area (~ 1 m as of 2017) exemplifies the association of relatively minor subsidence with relatively deep and weak swelling clay anomalies.

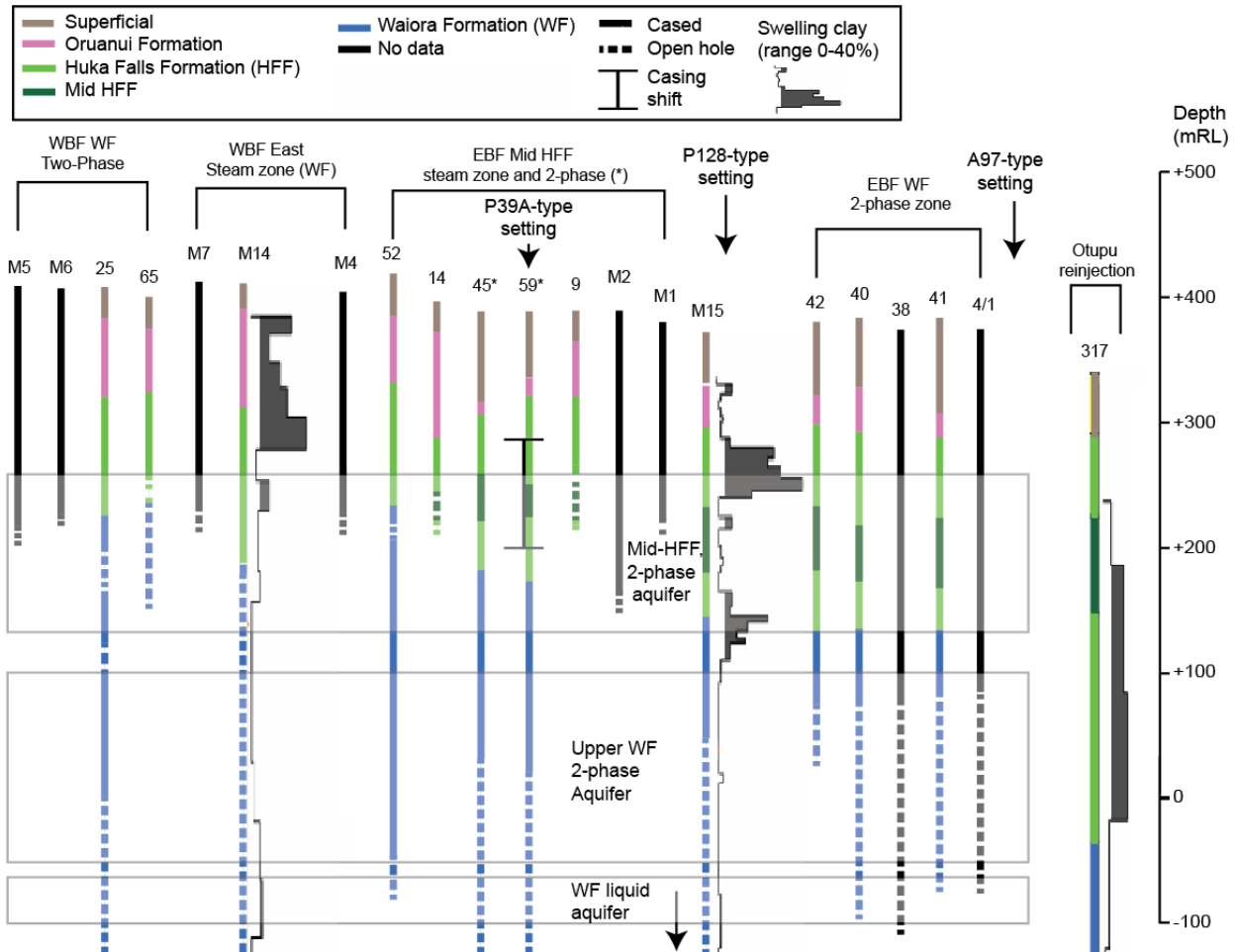


**Figure 5: Well geology, swelling clay, and casing information for selected WBF and EBF wells. Open hole = slotted liner, perforated liner or perforated casing.**

We summarize key reservoir observations as follows:

- HFF is laterally extensive across Wairakei-Tauhara (e.g. Rosenberg *et al.*, 2009);
- Pressure drawdown in the deep liquid reservoir (WF) was similarly evenly distributed across Wairakei-Tauhara (Bixley *et al.*, 2009);
- Swelling clay contents vary significantly laterally with swelling clay contents increasing with decreasing distance to areas of (past) discharge of chloride springs. These areas also tend to correlate with areas of high subsidence in Wairakei-Tauhara.

## 2.2 Levelling data and curve fitting

As discussed in Section 1, equation (1) combines a linear and exponential term to model level history. An asymmetric Multiple Sigmoidal (MS) curve is introduced in this study to match level observations. For the general case of  $k = 1, \dots, n$  subsidence events, our MS curve takes the form:

$$s(t) = 0 \quad t = 0$$

$$s(t) = \sum_{k=1}^n s_k^{max} \left[ 1 + \left( \frac{t_k^m - t_k^i}{t - t_k^i} \right)^{p_k} \right]^{-1}, \quad t > 0 \quad (3)$$

where  $s_k^{max}$  is the maximum subsidence of event  $k$  in meters,  $t_k^m$  and  $t_k^i$  are the middle and initial time of event  $k$  (during which pressure change is observed) respectively, with  $s(t_k^m) = 0.5 s_k^{max}$ , and  $p_k$  is a power factor ( $p_k \geq 1$ ) which controls the spreading of the subsidence over time in a similar way to constant  $T_l$  in equation (1). Although parameter  $s_k^{max}$  can be calibrated against pressure history (linear component of equation 1; Bromley, 2006), or narrowed down by trial and error, an empirical approach to selecting  $s_k^{max}$  values is proposed here that takes into account pressure change in combination with other reservoir information as follows:

$$s_k^{max} = H \cdot D_f \cdot P_k \cdot [C_s \cdot (1 - \phi) \cdot MeB_{max} + C_p \cdot \phi] \quad (4)$$

which is a dual compaction model with one component of subsidence related to porosity change and another component of subsidence related to change in rock volume (swelling clay water expel or swell-up), as conceptually portrayed in Figure 6.

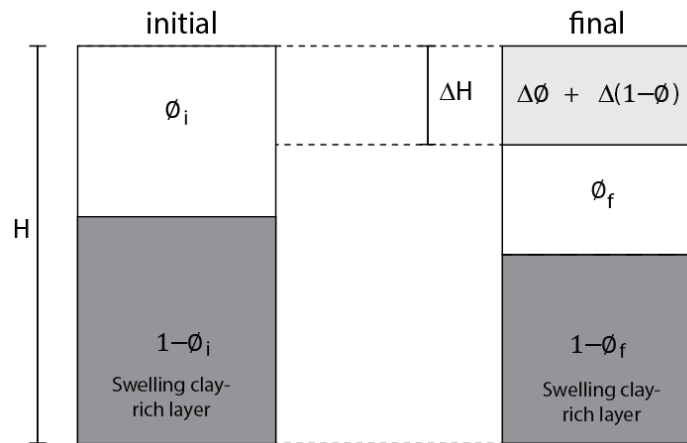


**Figure 6: Compaction model based on the concept of two components of subsidence: porosity ( $\phi$ )-related and swelling-clay related.**

Parameters in Equation 4 are defined as follows:

- $H$  = Thickness of compressible layer, defined as the depth interval with swelling clay  $> 5\%$  ;

- $\emptyset$  = porosity of the compressible layer (values used here: 50% in Upper HFF and 45% in Lower HFF);
- $P_k$  = pressure factor, defined as  $P_k = \Delta P_k / P_i$  where  $\Delta P_k$  is the pressure difference between the start and end of subsidence event  $k$ , and  $P_i$  is the initial (pre-exploitation) pressure at the average depth of the compressible layer. Pressure values are approximated from pressure history as in Figure 3;
- $D_f$  = depth factor (1 at surface and approaching zero with increasing depth) which approximates the effect of depth ( $D$ ) and thickness of the compressible layer(s) on the maximum value and shape of surface subsidence anomaly. Adapting Geertsma's model (Gertsma, 1973; Walsh, 2002), the following depth factor is used here:

$$D_f = 1 - \frac{D}{\sqrt{(D^2 + 5 \cdot H^2)}} \quad (5)$$

- $MeB_{max}$  = swelling clay content (%), defined as the maximum swelling clay content of the compressible layer from Methylene Blue tests;
- $C_s$  = compaction swelling clay factor, corresponding to the vertical strain  $\Delta H/H$  associated with volume change due to capture or expel of water into/from the swelling clay mineral structure;
- $C_p$  = compaction porosity factor, corresponding to the vertical strain  $\Delta H/H$  due to reduction of porosity. At Wairakei, assuming that a swelling clay-rich layer is also a weak layer, the compaction factor is assumed to approach unity for high-swelling clay (or more generally, weak, poorly consolidated) materials, and zero for low-swelling clay (or more generally, highly consolidated & hydrothermally indurated (e.g. silicification)) materials.

### 3. Results

Level benchmark history of the Wairakei Bowl is characterised using three selected benchmarks: benchmark A97 (southern edge of subsidence bowl), benchmark P128 (centre of subsidence bowl) and benchmark P39A (southern edge, near well WK059; Figure 1 for location). Pressure gradient and magnitude of change (Figure 3) is used to guide time parameters (as in Table 1). Following equation 4, constant pressure results in  $P_f = 0$ . Accordingly, the period from early-mid 1970's to late 1990's, of approximately constant pressure (Figure 3) is generally ignored. Based on swelling clay anomalies (Figure 5), two compressible layers are defined for benchmark P128 (Table 1).

Benchmark P39A (Figure 7) exemplifies the use of sigmoidal curve fitting to infer total subsidence (back-extrapolation). With an estimated cumulative subsidence of 2.78 m for the period 1958-2014 (from Figure 7), the cumulative casing coupling shift of ~2 m in the depth range 100-171 m (Figure 5) accounts for approximately two thirds of the total estimated subsidence in the P39A area. Assuming the linear trend 2.68 cm/m can be extrapolated with depth, the bottom of the compacting layer can be placed at ~204 mGL (182 mRL), which is close to the bottom of HFF layer (212 mGL, or 174 mRL in WK059) and also 16 meters deeper than the deepest casing obstructions (188 m). Note, notwithstanding the uncertainties around the estimated depth interval accommodating deformation (~100-200 mGL), this deformation interval can be correlated stratigraphically with the shallow swelling clay peaks in WKM14 and WKM15 (Figure 4).

Figure 7 shows that while a general reduction in subsidence rate with time is observed for all benchmarks, as dictated by general sigmoidal trends (e.g. Bromley, 2006), second-order variations in subsidence rate occur in association with pressure changes in the reservoir.

Period	Input parameters	Benchmark				
		A97	P39A	P128		
				Top layer	Bottom layer	Total
<b>Testing &amp; Early Production (pressure decline)</b>	$S_1^{max}$	1.8	0.9	5.5	4.0	0.9
	Power factor	2.0	2.7	3.3	3.4	3.0
	Start year	1952.0	1958.0	1952	1952.0	1952.0
	Mid year	1975.0	1982.0	1970.5	1970.0	1970.0
<b>Production II (pressure decline)</b>	$S_2^{max}$	4.6	2.1	10.7	9.3	1.8
	Power factor	2.0	2.7	3.3	3.4	3.0
	Start year	1959.0	1959.0	1959.0	1959.0	1959.0
	Mid year	1987.5	1994.5	1986.2	1985.5	1985.5
<b>Production III (pressure recovery)</b>	$S_3^{max}$	-0.2	0.2	-1.0	-0.1	-0.6
	Power factor	2.0	2.7	1.8	3.4	3.0
	Start year	1998.0	1995.0	1998.0	1998.0	1998.0
	Mid year	2010.0	2005.0	2010.0	2010.0	2010.0
<b>Production IV (pressure decline)</b>	$S_4^{max}$	0.3	0.2	1.1	0.3	0.6
	Power factor	2.0	2.7	1.8	3.4	3.0
	Start year	2012.0	2012.0	2012	2012.0	2012.0
	Mid year	2019.0	2019.0	2019	2017.0	2017.0

**Table 1: Benchmark curve fitting input parameters used in Figure 7.**

#### 4. Discussion and conceptual model

One key question to address in this study is the behavior of benchmark levels of the Wairakei Bowl, namely, benchmarks P128 and A97. These benchmarks appear to mimic, to variable extent, the pressure trends of the WF reservoir. Specifically:

1. Benchmark P128 shows a noticeable post-1998 reduction in subsidence rate compared to the pre-1998 period;
2. Benchmark A97 shows comparatively a much more subtle post-1998 reduction;
3. Both benchmarks show a slight increase in subsidence rate post-2012.

A refined conceptual model of subsidence is proposed to explain differential subsidence within the Wairakei subsidence bowl, the key elements of which are:

1. Hydrothermal swelling clay has a potentially amplifying effect on subsidence due to a control on both porosity and rock volume loss components of subsidence (Equation 4);
2. At the center of the subsidence bowl, two compacting layers are present with both layers seeing the effects of pressure recovery (this effect being greater in the bottom layer);
3. Both pressure decline and pressure recovery events in the WF propagated to HFF aquifers;
4. The variability of swelling clay content in the reservoir is explained by a combination of Upper and Lower HFF member spatial distribution, reservoir temperature and closeness to discharge of chloride springs, as portrayed in Figure 8.

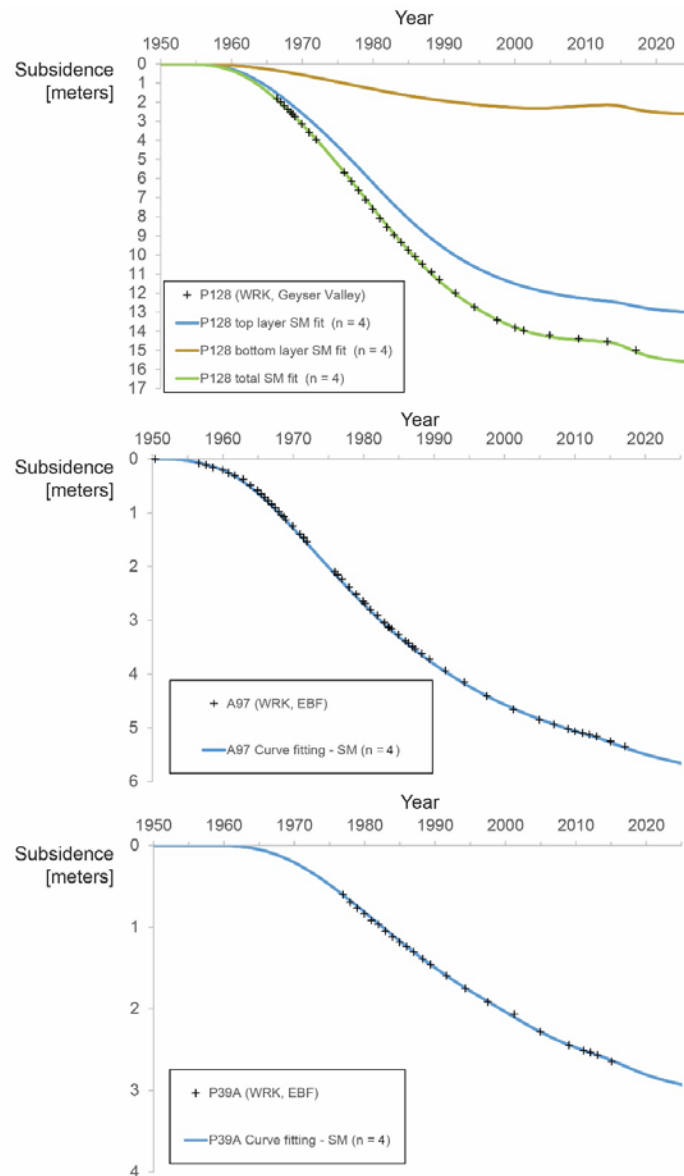


**Figure 7: Level history curve fitting for benchmarks P128, A97, and P39A, using fitted parameters from table 1 to equations 3 and 4.**

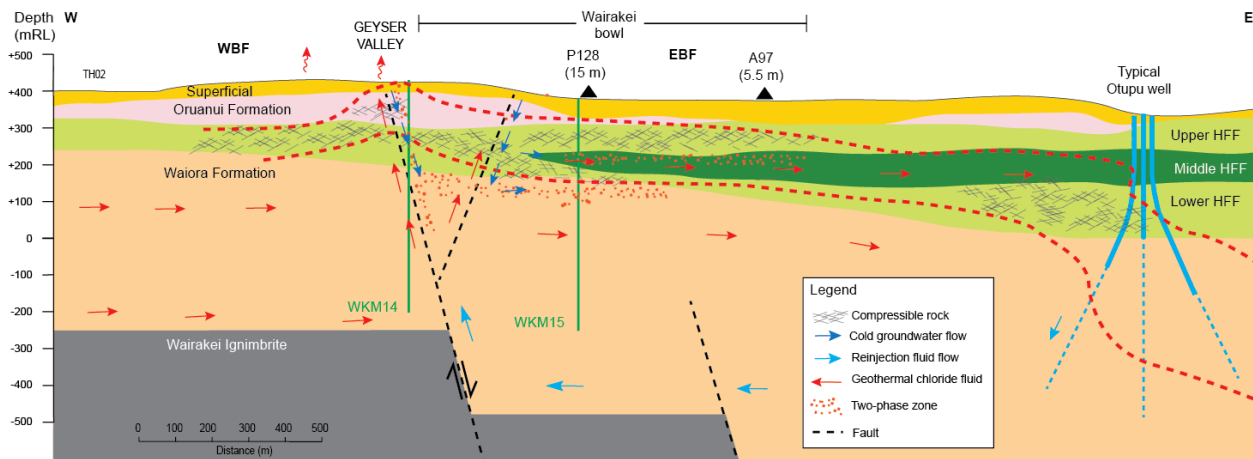


**Figure 8: Conceptual model of shallow stratigraphy in Wairakei bowl area (from west (left) to east (right)). 100°C and 220°C isotherms shown as red segmented lines.**

## 5. Concluding remarks

The availability of unprecedented level of detail (and reduced uncertainty) as to the thickness of the compaction zone from casing coupling shifts and swelling clay contents, are used to test a dual, swelling clay-controlled compaction model of subsidence. Based on the concept of Bromley (2016), the time-dependant component of subsidence is approximated by a sigmoidal curve, and the magnitude of the subsidence is approximated by means of a simple analytical relationship (equation 4) calibrated against field pressure history (Figure 3) and reservoir information (Figures 4 and Figure 5). It is found that the sigmoidal curve fitting presented in this study successfully replicate level trends for selected benchmarks of the Wairakei bowl.

## 6. Acknowledgments

The authors would like to thank Contact Energy Ltd for permission to publish data and Energy Surveys Ltd for levelling data collection and interpretation.

## REFERENCES

- Allis, R. (2000). Review of subsidence at Wairakei field, New Zealand. *Geothermics*, 29, 455-478.
- Allis, R., Bromley, C., & Currie, S. (2009). Update on subsidence at the Wairakei–Tauhara geothermal system, New Zealand. *Geothermics*, 38(1), 169-180.
- Allis, R. G., & Zhan, X. (2000). Predicting subsidence at Wairakei and Ohaaki geothermal fields, New Zealand. *Geothermics*, 29(4), 479-497.
- Bixley, P. F., Clotworthy, A. W., & Mannington, W. I. (2009). Evolution of the Wairakei geothermal reservoir during 50 years of production. *Geothermics*, 38(1), 145-154. doi:<https://doi.org/10.1016/j.geothermics.2008.12.007>.
- Brockbank, K., Bromley, C. J. and Glynn-Morris, T. 2011. Overview of the Wairakei-Tauhara Subsidence Investigation Program. Proceedings Stanford Geothermal Workshop.

- Bromley, C. (2006). Predicting subsidence in New Zealand geothermal fields: a novel approach. *GRC Transactions*, 30, 611-616.
- Bromley, C.; Currie, S.; Ramsay, G.; Rosenberg, M.; Pender, M.; O'Sullivan, M.; Lynne, B.; Lee, S-G.; Brockbank, K.; Glynn-Morris, T.; Mannington, W, Garvey, J. (2010). Tauhara Stage II Geothermal Project: Subsidence Report, GNS Science Consultancy Report 2010/151. 154p.
- Bromley C.J., Brockbank, K., Glynn-Morris T., Rosenberg, M., Pender M., O'Sullivan, M., Currie S., (2013), Geothermal subsidence study at Wairakei-Tauhara. *Journal of Geotechnical Engineering (Special Issue on Renewable Energy)* Vol. 166 Issue 2, p211-223. <http://www.icevirtuallibrary.com/content/article/10.1680/geng.12.00040>.
- Bromley, C., Currie, S., Jolly, S., Mannington, W. (2015) Subsidence: an Update on New Zealand Geothermal Deformation Observations and Mechanisms. *Proceedings WGC2015 Melbourne*, April 2015, #02021.
- Correa, N. A., Rae, A. J., Sepulveda, F. Distribution of Clay Minerals through a Conductive (MT) Zone on the Margins of a High-Temperature Geothermal Reservoir, Wairakei Geothermal Field, Taupo Volcanic Zone, New Zealand, *GRC Transactions*, 37, 459-462.
- Gunderson, R., Cumming, W., Astra, D., & Harvey, C. (2000). Analysis of smectite clays in geothermal drill cuttings by the methylene blue method: for well site geothermometry and resistivity sounding correlation. *Proceedings World Geothermal Congress*, Kyushu, Japan.
- Rosenberg, M. D., Bignall, G., & Rae, A. J. (2009). The geological framework of the Wairakei–Tauhara Geothermal System, New Zealand. *Geothermics*, 38(1), 72-84. doi:<http://dx.doi.org/10.1016/j.geothermics.2009.01.001>.
- Sepúlveda, F., Mannington, W., Charroy, J., Soengkono, S., Ussher, G (2012). Integrated approach to interpretation of magnetotelluric study at Wairakei, New Zealand. *Proceedings Stanford Geothermal Workshop*.
- Sepúlveda, F., Andrews, J., Kim, J., Siega, C. Milloy, S. F. (2015). Spatial-temporal Characteristics of Microseismicity (2009-2014) of the Wairakei Geothermal Field, New Zealand. *Proceedings WGC2015 Melbourne*, April 2015, #13047.
- Taylor, R. K. and Smith, T. J. (1986). *The Engineering Geology of Clay Minerals: Swelling, Shrinking and Mudrock Breakdown*. Clay Minerals, 21, 235, 260.
- Villar, M.V. and Lloret, A. (2004). Influence of temperature on the hydro-mechanical behaviour of a compacted bentonite. *Applied Clay Science*, 26, 337– 350
- White, P. A., & Hunt, T. M. (2005). Simple modelling of the effects of exploitation on hot springs, Geysir Valley, Wairakei, New Zealand. *Geothermics*, 34(2), 184-204. doi:<https://doi.org/10.1016/j.geothermics.2004.07.003>